

# In-plane deformation of cantilever plates with applications to lateral force microscopy

John E. Sader<sup>a)</sup> and Christopher P. Green

*Department of Mathematics and Statistics, University of Melbourne, Victoria, 3010 Australia*

(Received 15 August 2003; accepted 12 January 2004; published 10 March 2004)

The in-plane deformation of atomic force microscope (AFM) cantilevers under lateral loading is commonly assumed to have negligible effect in comparison to other deformation modes and ignored. In this article, we present a theoretical study of the behavior of cantilevers under lateral loading, and in so doing establish that in-plane deformation can strongly contribute to the total deformation, particularly for rectangular cantilevers of high aspect ratio (length/width). This has direct implications to lateral force microscopy, where the neglect of in-plane deformation can contribute to significant quantitative errors in force measurements and affect the interpretation of measurements. Consequently, criteria and approaches for minimizing the effects of in-plane deformation are presented, which will be of value to users and designers of AFM cantilevers. Accurate analytical formulas for the in-plane spring constants of both rectangular and V-shaped cantilevers are also presented. © 2004 American Institute of Physics. [DOI: 10.1063/1.1667252]

## I. INTRODUCTION

Knowledge of the deformation of atomic force microscope (AFM) cantilevers is fundamental to the performance of the instrument and the interpretation of measurements. In lateral force microscopy,<sup>1</sup> a lateral load is applied to the imaging tip of the cantilever, inducing a moment about the cantilever axis. The resulting rotational deformation (twisting) of the cantilever, which is typically measured by the optical deflection technique, can then be used to determine the applied lateral force. This is typically accomplished by (i) knowledge of the torsional spring constant and calibration of the lateral displacement of the imaging tip,<sup>2-5</sup> or (ii) direct calibration of lateral forces acting on the cantilever.<sup>6,7</sup>

It is commonly assumed that AFM cantilevers are resistant to in-plane deformation, i.e., deformation parallel to the plane of the cantilever, which is induced by the application of a lateral force to the imaging tip. This assumption of pure rotation then enables the rotational deformation to be related directly to the lateral movement of the tip. Indeed, the measurement approach mentioned in (i) above is contingent on this premise. Consequently, in this article we present a detailed theoretical study of the effects of in-plane deformation in AFM cantilevers. Both rectangular and V-shaped cantilevers are considered, since these are used predominantly in practice. In so doing, we establish that in-plane deformation can strongly contribute to the total deformation, particularly for practical rectangular cantilevers of high aspect ratio (length/width). We also present rigorous conditions under which in-plane deformation of cantilevers can be neglected. This is particularly relevant to lateral force measurements, where the assumption of pure rotation underlies the theoretical framework of the above experimental methodology.<sup>2-5</sup> We emphasize that even though the optical deflection tech-

nique is insensitive to in-plane movement of the cantilever, such in-plane movement can strongly affect the interpretation of measurements, and hence quantitative lateral force results, as we shall discuss.

The presentation of this article is as follows. We will commence by deriving analytical formulas for the in-plane spring constants of both rectangular and V-shaped cantilevers. We primarily consider deformation perpendicular to the cantilever symmetry axis, since this is the case most commonly encountered in practice. For completeness, the complementary case of loading parallel to the symmetry axis of the cantilever is given in the Appendix. Following this, the effects of rotation on the total deformation shall be included. In so doing, we shall present criteria that ensure the effects of in-plane deformation are negligible. Finally, we will present a discussion of the implications of these results to lateral force measurements and to a recent study by one of the authors which compared the lateral stability of rectangular and V-shaped cantilevers.<sup>8</sup>

## II. THEORY

In this section, we examine the effects of in-plane deformation under the application of lateral forces, for both rectangular and V-shaped cantilevers, schematics of which are given in Fig. 1. We focus on loading in the  $y$  direction only, see Fig. 2, for reasons given above; results for loading in the  $x$  direction are given in the Appendix. Note that a general lateral load is easily constructed using a linear combination of these results. Initially, we consider the resulting in-plane deformation only, as illustrated in Fig. 3, i.e., deformation of the cantilever in the  $x$ - $y$  plane. The combined effects of rotational and in-plane deformation will be examined subsequently.<sup>9</sup> The subscripts  $x$  and  $y$  shall refer to loading in the  $x$  and  $y$  directions, respectively.

Throughout, the load is applied at the end of the imaging tip, at a distance  $\Delta L$  measured back from the end-tip of the

<sup>a)</sup>Electronic mail: jsader@unimelb.edu.au

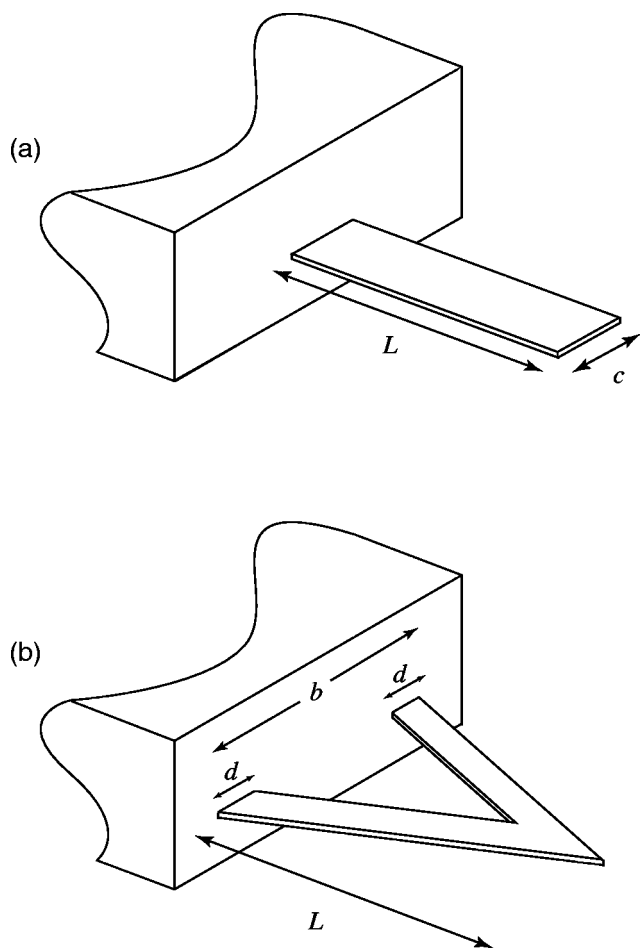


FIG. 1. Schematic diagram of (a) rectangular and (b) V-shaped cantilever plates showing dimensions.

cantilever, along its axis of symmetry, see Fig. 2. We note that the imaging tip has the effect of making the cantilever rigid at its position. Consequently, the portion of the cantilever between the imaging tip and the end of the cantilever is taken to be rigid in the following calculations.<sup>8</sup>

**A. In-plane deformation**

Lateral loading in the *y* direction corresponds to loading perpendicular to the symmetry axis of the cantilever. We now

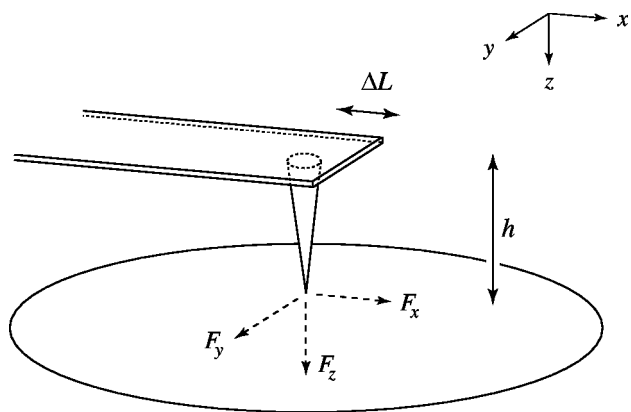


FIG. 2. Schematic of cantilever tip showing applied forces  $F_x, F_y, F_z$ , load position  $\Delta L$  on the cantilever, height of imaging tip  $h$  measured from the base of the tip to the midplane of the cantilever, and coordinate system used. Origin of coordinate system is at the center of mass of the clamped end of the plate.

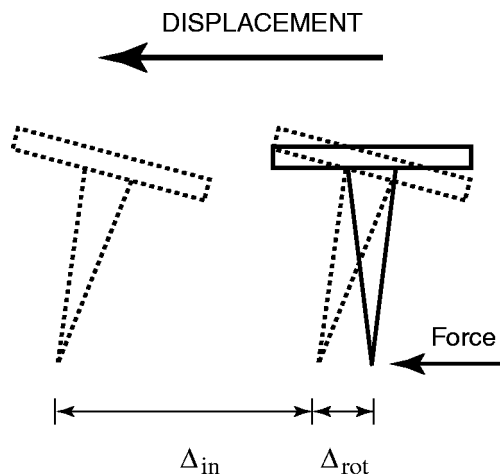


FIG. 3. Graphical illustration of tip deformation resulting from a lateral load: undeformed cantilever (solid), deformed cantilever (dashed). Displacement due to pure rotational deformation is  $\Delta_{rot}$ . Displacement due to pure in-plane deformation is  $\Delta_{in}$ . Total displacement of tip is given by sum of  $\Delta_{rot}$  and  $\Delta_{in}$ .

derive simple analytical formulas for the in-plane spring constants of both rectangular and V-shaped cantilevers under such loading. The accuracy and validity of these formulas will be assessed by comparison to rigorous finite element results below.

For rectangular cantilevers, we work in the limit where the length  $L$  of the cantilever greatly exceeds its width  $c$ . Consequently, standard beam theory<sup>10</sup> is applicable, from which we obtain the well-known result

$$k_y = \frac{Etc^3}{4(L - \Delta L)^3}, \tag{1}$$

where the in-plane spring constant  $k_y$  is defined as the ratio of the applied lateral force to the resulting in-plane displacement at the load point, and where  $E$  is Young’s modulus,  $t$  is the thickness of the plate, and all other dimensions are specified in Fig. 1(a).

To analyze the V-shaped cantilever, we consider the limit of  $d/b=0.5$  which corresponds to a triangular plate. Since the lateral load is perpendicular to the symmetry axis of the cantilever, the stress distribution must be antisymmetric about this symmetry axis, i.e., compressive on one side of the symmetry axis, and tensile on the other. Furthermore, the stress will be largest near the outer edge of the cantilever, and decrease towards the symmetry axis. It then follows that removing a triangular section near the center of the triangle, which is equivalent to reducing the arm width ratio  $d/b$ , will have little effect on the spring constant. Consequently, the in-plane spring constant of a V-shaped cantilever will be independent of the arm width ratio  $d/b$ , to leading order, and well approximated by that of a solid triangle. We therefore utilize the analytical solution in Ref. 11 for an infinite wedge loaded at its end-tip and restrained at a distance  $L$  from the end-tip, along the symmetry axis,

$$k_y = Et(\alpha - \sin \alpha \cos \alpha) \left[ \ln \left( \frac{L}{\Delta L} \right) \right]^{-1}, \tag{2}$$

where

$$\alpha = \tan^{-1}\left(\frac{b}{2L}\right). \tag{3}$$

This solution will be valid for loads positioned away from the end-tip of the cantilever, i.e., finite  $\Delta L/L$ , provided this ratio is small, as the true stress distribution will be accurately represented.

Note that the above in-plane spring constant of a V-shaped cantilever is independent of the arm width  $d$ , whereas the corresponding spring constant for a rectangular cantilever is strongly dependent on its width  $c$ .

**B. Combination of rotational and in-plane deformation**

We now examine the combined effect of in-plane and rotational deformations, when lateral forces are applied to the imaging tip, see Fig. 3. To this end, we utilize the in-plane formulas presented above and established analytical formulas for the rotational spring constants of rectangular<sup>10,12</sup> and V-shaped cantilevers,<sup>13</sup> which are reviewed in Ref. 8.

To begin, we note that application of a lateral force to the end of the imaging tip will result in both a rotational deformation and in-plane movement of the cantilever, see Fig. 3. To account for both contributing effects, we add the lateral displacements resulting from these deformations to give the total lateral spring constant  $k$ ,

$$k = k^{\text{rot}}(1 + \varepsilon)^{-1}, \tag{4}$$

where

$$\varepsilon = \frac{k^{\text{rot}}}{k^{\text{in}}}, \tag{5}$$

where the superscripts “rot” and “in” refer to individual contributions for pure rotational and in-plane deformations, respectively. Specifically,  $k^{\text{rot}}$  is the ratio of applied lateral force to the lateral displacement at the load point, for the case of pure rotational deformation of the cantilever. In contrast,  $k^{\text{in}}$  is the analogous spring constant for pure in-plane deformation of the cantilever. Importantly, if the spring constant due to in-plane deformation  $k^{\text{in}}$  greatly exceeds that due to rotational deformation  $k^{\text{rot}}$ , i.e.,  $\varepsilon \ll 1$ , then deformation of the tip is purely due to rotational movement of the cantilever.

For a rectangular cantilever loaded in the  $y$  direction, we find<sup>12</sup>

$$\varepsilon_y = \frac{2}{3(1 + \nu)} \left(\frac{t}{h}\right)^2 \left(\frac{L - \Delta L}{c}\right)^2, \tag{6}$$

where  $h$  is the imaging tip height, see Fig. 2.

For V-shaped cantilevers, the corresponding expression is considerably more complex. We therefore simply present the leading order scaling behavior, which can be easily derived from the formulas given above and in Ref. 8, namely

$$\varepsilon_y \sim O\left(\left[\frac{d}{b}\right]\left[\frac{t}{h}\right]^2\left[\frac{L}{b}\right]^2\right). \tag{7}$$

It is important to note that  $\varepsilon_y$  depends strongly on all dimensions of the cantilevers, including their plan view geom-

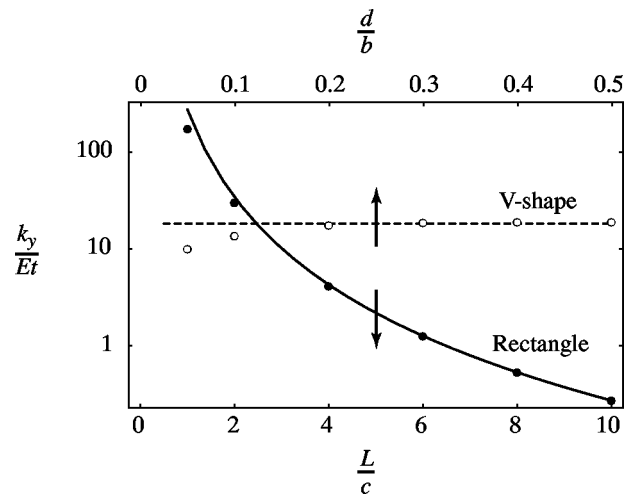


FIG. 4. Comparison of analytical and FE results for the in-plane lateral spring constants  $k_y$  of rectangular and V-shaped cantilevers for  $\Delta L/L = 0.03$ . Analytical formula Eq. (1) for rectangular cantilever (solid line). Analytical formula Eq. (2) for V-shaped cantilever (dashed line). FE results for rectangular cantilever (solid circles). FE results for V-shaped cantilever (open circles).

etries. This is in direct contrast to loading in the  $x$  direction, where  $\varepsilon_x \sim O(t/h)^2$  for both rectangular and V-shaped cantilevers.

Note that in all cases, the relative importance of in-plane deformation decreases as the imaging tip height  $h$  increases. The performance of rectangular and V-shaped cantilevers with respect to in-plane deformation shall be examined in detail in the following section.

**III. RESULTS AND DISCUSSION**

To begin, we assess the validity and accuracy of the formulas presented in Sec. II A for the in-plane spring constants, by presenting a comparison with finite element (FE) analysis.<sup>14</sup> Since the cantilever thickness is typically much smaller than its plan view dimensions, in-plane deformation inherently occurs under plane stress conditions; this is utilized in the FE analysis. In addition, we only present results for V-shaped cantilevers with an aspect ratio  $b/L = 1$ , which corresponds to the typical practical case; similar results are obtained for  $0.5 \leq b/L \leq 1.5$ . Similarly, we only present results for imaging tips positioned at  $\Delta L/L = 0.03$ ; results obtained for values within the range  $0.01 \leq \Delta L/L \leq 0.1$  exhibit identical behavior and accuracy. Results for Poisson’s ratio  $\nu = 0.25$  are given only, since the in-plane spring constants are very weakly dependent on Poisson’s ratio. Also note the following typical geometric properties of AFM cantilevers: (i) V-shaped cantilever arm width ratios:  $0.1 \leq d/b \leq 0.3$ ; (ii) rectangular cantilever aspect ratios,  $2 \leq L/c \leq 10$ ; (iii) position of the imaging tip for both types of cantilevers,  $0.01 \leq \Delta L/L \leq 0.1$ ; and (iv) ratio of the imaging tip height to the cantilever thickness,  $5 \leq h/t \leq 30$ . These parameter ranges will be used in the pursuing discussion.

**A. In-plane deformation**

In Fig. 4, we present a comparison of the in-plane spring constants derived in Sec. II A with results obtained using FE

analysis, for the case of loading in the  $y$  direction. Both rectangular and V-shaped cantilevers are considered. From Fig. 4, it is clear that the analytical formulas accurately capture the behavior of the cantilevers. In particular, we find that the in-plane spring constant of a V-shaped cantilever is relatively insensitive to the arm width ratio  $d/b$ , as predicted in Eq. (2); this is particularly true for  $d/b > 0.2$ . This insensitivity to cantilever plan view geometry contrasts directly with the behavior of rectangular cantilevers, whose in-plane spring constant is strongly dependent on the aspect ratio  $L/c$ . We also note that the formulas presented in the Appendix for loading in the  $x$  direction exhibit similar accuracy, although the dependence on geometry is very different.

It is interesting to compare the relative performance of V-shaped and rectangular cantilevers to in-plane deformation, under conditions where their normal spring constants (for loading in the  $z$  direction, see Fig. 2) are equal.<sup>8</sup> Specifically, we choose the cantilevers to have identical lengths, thickness, and material properties. This enables the relative merits of these cantilevers, with respect to in-plane deformation, to be examined properly. We ensure that both cantilevers have equal normal spring constants by invoking the parallel beam approximation,<sup>15</sup> which dictates the relationship between the width of the arms of both cantilevers,

$$c = 2\bar{d} \left\{ 1 + \frac{4\bar{d}^3}{b^3} \right\}^{-1}, \quad (8)$$

where  $\bar{d} = d \cos \alpha$  is the shortest width across the arms of the V-shaped cantilever. From Fig. 4, we find that the relative performance of the cantilevers is strongly dependent on their plan view geometry. For rectangular cantilevers with  $L/c > 2$ , corresponding to equivalent V-shaped cantilevers with  $d/b < 0.3$ , Fig. 4 establishes that V-shaped cantilevers possess higher in-plane spring constants in the  $y$  direction. It is important to note, however, that for  $d/b = 0.3$ , which corresponds to the upper limit of arm width ratios encountered in practice, equivalent V-shaped and rectangular cantilevers give comparable  $y$  direction in-plane spring constants. These results contrast to those in the  $x$  direction, where the equivalent rectangular and V-shaped cantilevers exhibit similar in-plane spring constants, regardless of their plan view geometry.

We emphasize that these findings for in-plane deformation are independent of those for pure rotational deformation found in Ref. 8, which showed that rectangular cantilevers exhibit superior resistance. The implications of combining these independent findings for rotational and in-plane deformation will be discussed below.

## B. Implications to total lateral deformation

In practice, lateral loading of AFM cantilevers is typically achieved by application of forces to the imaging tip, see Fig. 2. Consequently, both rotational deformation of the cantilever, due to induced moments, and in-plane deformation must be included to determine the total cantilever deformation.<sup>9</sup> In Sec. IIB, formulas for the lateral spring constants were given, which include the combined effects of rotational and in-plane deformation, and thus indicate the

relative importance of these deformations. Since the formulas derived in Sec. II exhibit good accuracy, we now use these results to investigate the total lateral performance of AFM cantilevers.

First, we note that AFM cantilevers possess imaging tips with the property that their height greatly exceeds the cantilever thickness, i.e.,  $h/t \gg 1$ . It then follows that both rectangular and V-shaped cantilevers are insensitive to in-plane deformation in the  $x$  direction, since  $\varepsilon_x \sim O(t/h)^2 \ll 1$ . Next, we consider loading in the  $y$  direction. For V-shaped cantilevers encountered in practice, we again find  $\varepsilon_y \ll 1$ , since the aspect ratio of the cantilevers  $b/L \sim 1$  and  $d/b < 1$ , see Eq. (7). Combined with the above result, this establishes that practical V-shaped cantilevers are insensitive to in-plane deformation in both the  $x$  and  $y$  directions, and thus all directions. However, the situation is very different for rectangular cantilevers. From Eq. (6), we see that there are competing terms in  $\varepsilon_y$ , which allow for the possibility that  $\varepsilon_y$  is order unity. This can occur for cantilevers of high aspect ratio  $L/c$  and small to moderate imaging tip ratio  $h/t$ , e.g., for  $h/t = 5$ ,  $L/c = 10$ , and  $\nu = 0.25$ , we find  $\varepsilon_y \sim 2$ , which indicates that lateral movement of the tip due to in-plane deformation of the cantilever is twice as large as that due to rotation of the cantilever. Indeed, many rectangular cantilevers currently manufactured possess the property  $\varepsilon_y \sim O(1)$ . This finding can have significant implications to quantitative force studies performed using lateral force microscopy, as we shall now discuss.

In lateral force microscopy, lateral forces are typically measured in the  $y$  direction. In performing these measurements, the cantilever sensitivity to lateral forces must be calibrated. One method used is to bring the imaging tip into contact with a surface, then move the surface and induce a prescribed lateral displacement of the tip. When measured using the optical deflection technique, this is observed as a change in the photodiode voltage. Consequently, a relationship between the lateral displacement of the tip and the photodiode voltage is established. Throughout, it is assumed that this lateral displacement of the tip induces a pure rotation of the cantilever. This enables use of the torsional spring constant to connect the measured lateral displacement of the tip to the applied lateral force, once the imaging tip height is known. However, if significant in-plane deformation occurs, then use of the torsional spring constant to connect the lateral force to the lateral displacement of the tip will not be valid.

Rectangular cantilevers are used commonly in lateral force measurements for a number of reasons, which include their simplicity of design, calibration, and relative insensitivity to load position in comparison to V-shaped cantilevers.<sup>1</sup> Use of rectangular cantilevers that satisfy the criterion

$$\varepsilon_y = \frac{2}{3(1+\nu)} \left( \frac{t}{h} \right)^2 \left( \frac{L - \Delta L}{c} \right)^2 \ll 1, \quad (9)$$

will ensure that the foundations of the above-mentioned methodology for quantitative lateral force measurements remain valid. Alternatively, effects of in-plane deformation can be rigorously included using the theoretical formalism given above.

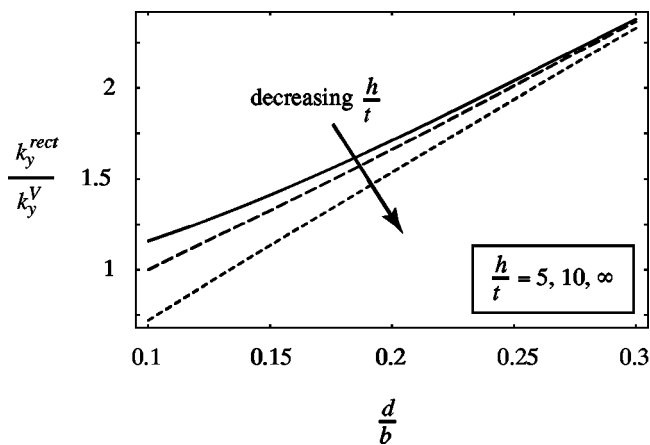


FIG. 5. Plot showing ratio of lateral spring constants of equivalent rectangular and V-shaped cantilevers, as a function of V-shaped geometry, for lateral loading in the  $y$  direction. Both types of cantilevers have identical normal spring constants, lengths, imaging tip positions, and tip heights, as specified in Ref. 8, also see Eq. (8). Superscripts rect and V refer to rectangular and V-shaped cantilevers, respectively. Results given for  $b/L=1$ ,  $\Delta L/L=0.03$ ,  $\nu=0.25$ , and for various tip ratios  $h/t=5, 10, \infty$ . Note that  $h/t \rightarrow \infty$  corresponds to results given in Ref. 8 for pure rotational deformation.

We emphasize, that the effects of in-plane deformation are in addition to other complicating factors such as tip-sample compliance,<sup>16</sup> and imaging tip deformation,<sup>17</sup> which can all strongly affect the calibration and interpretation of lateral force measurements. Importantly, the influence of these effects can be eliminated by directly calibrating the angle of rotation of the cantilever, rather than the displacement of the tip. In such cases, use of the torsional spring constant to determine the lateral force is formally valid, since the applied torque is independent of the above factors. Procedures that directly calibrate lateral forces acting on the tip<sup>6,7</sup> are also valid, regardless of in-plane deformation of the cantilever.

Finally, we investigate the inclusion of these findings into a recent study<sup>8</sup> by one of the authors, which compared the lateral stability of rectangular and V-shaped cantilevers. Specifically, that study considered pure rotational deformation, to examine the premise that V-shaped cantilevers are more resistant to twisting, and hence the effects of lateral forces, than rectangular cantilevers. In so doing, Ref. 8 formally established that rectangular cantilevers are more resistant to rotational deformation than V-shaped cantilevers. This has significant implications in practice, since V-shaped cantilevers are used commonly due to their presumed superior resistance to rotational deformation, and in-plane deformations cannot be measured typically. We now include in-plane deformation, and examine any implications to the lateral stability resulting from both rotational and in-plane deformation. Only lateral deformations in the  $y$  direction are considered, since both types of cantilevers are insensitive to in-plane deformations in the  $x$  direction, i.e., results presented in Ref. 8 for lateral stability in the  $x$  direction are not influenced by the effects of in-plane deformation.

A comparison of rectangular and V-shaped cantilevers, which shows the effects of in-plane deformation on lateral stability in the  $y$  direction, is given in Fig. 5 for the typical

range of  $0.1 \leq d/b \leq 0.3$  (which corresponds to  $6 \geq L/c \geq 2$  for the equivalent rectangular cantilever) and  $\Delta L/L=0.03$ ; similar results are obtained for  $0.01 \leq \Delta L/L \leq 0.1$ . These results indicate that the effects of in-plane deformation in the comparison of V-shaped and rectangular cantilevers, are enhanced by reducing the arm widths and imaging tip heights of the cantilevers, and can be significant for small tip height ratios  $h/t$  and small arm width ratios  $d/b$ . Importantly, a survey of V-shaped cantilevers currently available reveals that at most, in-plane deformation is comparable to rotational deformation in the equivalent rectangular cantilever.<sup>18</sup> This leads to the comparable rectangular cantilever exhibiting a lateral spring constant approximately half that of the V-shaped cantilever;<sup>18</sup> this occurs only for small  $h/t$  and  $d/b$ . Apart from these limiting cases, rotational deformation captures the dominant behavior and results in rectangular cantilevers exhibiting superior resistance to lateral forces,<sup>19</sup> as shown in Ref. 8.

The findings of this study and Ref. 8 establish that rectangular and V-shaped cantilevers exhibit lateral stiffness of comparable order, with rectangular cantilevers generally exhibiting superior lateral resistance. Since the lateral and normal spring constants of both types of cantilevers are sensitive to cantilever dimensions and can be easily tuned, use of V-shaped cantilevers on the grounds that they exhibit superior resistance to lateral forces, as is currently the case, is not justifiable. This conclusion is further supported by the geometric complexity of V-shaped cantilevers, which can complicate the interpretation and calibration of measurements.

This study has investigated the effects of in-plane deformation on the total lateral deformation of both rectangular and V-shaped cantilevers. In so doing, we examined the validity of the assumption that in-plane cantilever deformation is negligible in comparison to rotational deformation. We found that the validity of this commonly held premise depends on the direction of loading and the cantilever under consideration. When loaded at the imaging tip, this assumption is valid for V-shaped cantilevers always, irrespective of the cantilever geometry and direction of loading. For rectangular cantilevers, however, this conclusion holds for loading in the  $x$  direction only. For loading in the  $y$  direction, the relative importance of in-plane and rotational deformation in rectangular cantilevers is strongly dependent on the cantilever geometry. Subsequently, a simple criterion was formulated, which when satisfied, ensures that in-plane deformation is negligible in comparison to rotational deformation. This is expected to be of particular importance in lateral force measurements, where the assumption of pure rotational deformation underlies conventional experimental methodology. The findings of this study will therefore be of value to the users and designers of AFM cantilevers.

## ACKNOWLEDGMENTS

This research was supported by the Particulate Fluids Processing Center of the Australian Research Council and by the Australian Research Council Grants Scheme. C.P.G. acknowledges support from an Australian Postgraduate Award.

**APPENDIX**

In this Appendix, we derive analytical formulas for the in-plane spring constants of rectangular and V-shaped cantilever in the  $x$  direction, which corresponds to loading along the symmetry axis of the cantilever. These formulas exhibit similar accuracy to those for the  $y$  direction derived in Sec. II A.

For a rectangular cantilever, we consider the limiting case where its length  $L$  is much greater than its width  $c$ . A simple analytical formula is then obtained by noting that a load parallel to the symmetry axis of the cantilever induces uniform stresses parallel to the direction of loading. Consequently, the spring constant  $k_x$  in this direction, is given by

$$k_x = \frac{Etc}{L - \Delta L}, \tag{A1}$$

where  $E$  is Young's modulus,  $t$  is the thickness of the plate, and all other dimensions are specified in Fig. 1(a).

Analysis of the V-shaped cantilever is more complicated due to its elaborate geometry. We model this cantilever by dividing it into two sections, as in Ref. 13. The first is a solid triangle at the end of the cantilever, and the second is two supporting skewed rectangular arms. A straight line running parallel to the clamped end, at a distance of  $L(1 - 2d/b)$  from the clamped end, separates these two sections. This then enables solutions for both sections to be evaluated separately, and later combined to give the total spring constant for the cantilever.

For the triangular end section, we utilize the exact analytical result given in Ref. 11 for the in-plane deformation of an infinite wedge at its end point,

$$w_1 = \frac{F_x}{Et(\alpha + \sin \alpha \cos \alpha)} \ln\left(\frac{L}{\Delta L} \frac{2d}{b}\right), \tag{A2}$$

where  $\alpha$  is defined in Eq. (3),  $w_1$  is the displacement of the imaging tip relative to the bottom of the triangular section, along the symmetry axis,  $F_x$  is the applied lateral load, and all dimensions are as specified in Figs. 1(b) and 2. Provided  $\Delta L/L \ll 1$ , this limiting solution<sup>11</sup> will be a good approximation, since the true stress distribution will be well represented.

To calculate the deformation of the skewed rectangular arms, we note that the lateral load applied to the imaging tip is also applied to the top of these arms. In the case where the width of these arms is far smaller than their length, the problem then reduces to calculating the deflection of two attached beams, under the application of a concentrated force at their ends. The solution to this problem is<sup>11</sup>

$$w_2 = \frac{F_x L}{2E dt} \left(1 - \frac{2d}{b}\right) \sec^4 \alpha, \tag{A3}$$

where  $w_2$  is the displacement of the arms in the  $x$  direction relative to the clamped end.

Summing the contributions from Eqs. (A2) and (A3) then gives the total in-plane displacement of the cantilever at its imaging tip position. The resulting spring constant is therefore

$$k_x = \frac{2E dt}{L} \left( \left(1 - \frac{2d}{b}\right) \sec^4 \alpha + \frac{2}{(\alpha + \sin \alpha \cos \alpha)} \frac{d}{L} \ln\left(\frac{L}{\Delta L} \frac{2d}{b}\right) \right)^{-1}. \tag{A4}$$

Equations (A1) and (A4) clearly indicate that the in-plane spring constants in the  $x$  direction of both rectangular and V-shaped cantilevers decrease as the width of their respective arms decrease, i.e., width  $c$  for rectangular cantilevers, and width  $d$  for V-shaped cantilevers.

<sup>1</sup>E. Meyer, R. M. Overney, K. Dransfeld, and T. Gyalog, *Nanoscience: Friction and Rheology on the Nanometer Scale* (World Scientific, Singapore, 1998).

<sup>2</sup>Y. Liu, T. Wu, and D. F. Evans, *Langmuir* **10**, 2241 (1994).

<sup>3</sup>O. Pietrement, J. L. Beaudoin, and M. Troyon, *Tribol. Lett.* **7**, 213 (1999).

<sup>4</sup>R. G. Cain, S. Biggs, and N. W. Page, *J. Colloid Interface Sci.* **227**, 55 (2000).

<sup>5</sup>S. Ecke, R. Raiteri, E. Bonaccorso, C. Reiner, H.-J. Deiseroth, and H.-J. Butt, *Rev. Sci. Instrum.* **72**, 4164 (2001).

<sup>6</sup>D. F. Ogletree, R. W. Carpick, and M. Salmeron, *Rev. Sci. Instrum.* **67**, 3298 (1996).

<sup>7</sup>A. Feiler, P. Attard, and I. Larson, *Rev. Sci. Instrum.* **71**, 2746 (2000).

<sup>8</sup>J. E. Sader, *Rev. Sci. Instrum.* **74**, 2438 (2003).

<sup>9</sup>Throughout, we delineate between cantilever deformation and imaging tip deformation.

<sup>10</sup>R. J. Roark and W. C. Young, *Formulas for Stress and Strain* (McGraw-Hill, New York, 1975).

<sup>11</sup>S. Timoshenko, *Strength of Materials* (Van Nostrand, New York, 1955).

<sup>12</sup>For rectangular cantilevers, we neglect the higher order correction that accounts for the inherent restraint against axial warping of the plate (Ref. 8). This was included in Ref. 8 to ensure formulas for all spring constants possessed similar accuracy. The neglect of this term here ensures consistency with the derived in-plane spring constant, which neglects all higher order corrections. For aspect ratios  $L/c > 2$ , the maximum effect of this correction is a 30% increase in the torsional spring constant. This effect decreases as the aspect ratio increases (Ref. 8).

<sup>13</sup>J. W. Neumeister and W. A. Ducker, *Rev. Sci. Instrum.* **65**, 2527 (1994).

<sup>14</sup>LUSAS is a trademark of, and is available from FEA Ltd. Forge House, 66 High Street, Kingston Upon Thames, Surrey, KT1 1HN, UK. Plane stress elements with quadratic interpolation were used throughout. The number of elements was refined to ensure accuracy better than 1%. Quadrilateral elements were used for the rectangular cantilevers. For the V-shaped cantilevers, quadrilateral elements were used along the skewed rectangular arms, and triangular elements were used in the triangular end section.

<sup>15</sup>J. E. Sader, *Rev. Sci. Instrum.* **66**, 4583 (1995).

<sup>16</sup>R. W. Carpick, D. F. Ogletree, and M. Salmeron, *Appl. Phys. Lett.* **70**, 1548 (1997).

<sup>17</sup>M. A. Lantz, S. J. O'Shea, C. F. Hoole, and M. E. Welland, *Appl. Phys. Lett.* **70**, 970 (1997).

<sup>18</sup>This only occurs for V-shaped cantilevers with small arm width ratio  $d/b$ . For example, the V-shaped cantilever (Microlevers) by Veeco, 112 Robin Hill Road, Santa Barbara, CA 93117, with dimensions  $L = 323 \mu\text{m}$ ,  $b = 215 \mu\text{m}$ ,  $d = 21 \mu\text{m}$ ,  $h/t = 5.5$ , has an equivalent rectangular cantilever of aspect ratio  $L/c = 8$  with  $\epsilon_y \sim 1$ . The lateral stiffness of the equivalent rectangular cantilever is 0.6 times lower than the V-shaped cantilever.

<sup>19</sup>We note that any imaging tip deformation (Ref. 17) will reduce the difference between the lateral spring constants of the V-shaped and rectangular cantilever/tip combinations, provided the same tip is attached to both cantilevers.